Thermal and economic evaluation of thermocline combined sensible-latent heat thermal energy storage system for medium temperature applications☆

N. Ahmed[a], K.E. Elfeky[a], Lin Lu[b], Q.W. Wang[a],*

[a] Key Laboratory of Thermo-Fluid Science and Engineering, MOE, Xi'an Jiaotong University, Xi'an, Shaanxi 710049, China
[b] Department of Building Services Engineering, The Hong Kong Polytechnic University, Hung Hom, Kowloon, Hong Kong, China

ARTICLE INFO

ABSTRACT

In the current work a new thermocline combined sensible-latent heat thermal energy storage configuration is proposed as an alternative to the currently used thermal storage systems; containing solid rod structures of cheap naturally occurring material with phase change material capsules impregnated between the rods. An energy balance method coupled with an enthalpy based technique are used to develop a comprehensive transient numerical model. The numerical simulations are performed to compare the performance and the cost of the three types of thermal energy storage systems. The three thermal energy storage systems are; sensible rod structure, encapsulated phase change material and combined sensible-latent heat. The influence of different evaluation indexes on economic feasibility and the performance of thermal energy storage such as capital cost, capacity cost per kWh, axial temperature distribution, pumping work, thermocline degradation, effective discharging time and effective discharging efficiency; are analyzed. The results show that effective discharging efficiency and capacity costs for encapsulated phase change material, combined sensible-latent heat, sensible rod structure are 95%, 87%, 76% and \$42/kWh, \$37/kWh, \$35/kWh, respectively. Moreover, the hybrid configuration exhibits a storage capacity of 78.5 kWh/m^3, which is 26% higher than sensible rod structure and 22% lower than encapsulated phase change material configuration. The results of the comparative study indicate that the combined sensible-latent heat TES system seems to be a more viable option among the considered configurations due to its optimized performance and comparatively low cost. Also due to the reasons that thermal ratcheting of the storage tank is avoided and it provides stable fluid outlet temperature.

1. Introduction

The hazardous effects on the environment due to carbon emissions and high energy costs have triggered the need for the development and deployment of sustainable energy technologies with a particular focus on integration whenever possible [1]. Harnessing maximum solar thermal energy [2] and entrapping waste energy from industrial waste heat recovery processes [3]; are considered as potential alternate energy sources. However, the intermittent nature of these potential energy resources justifies the development of an efficient and cost effective TES [4]. Thus, the role of a TES is very critical to overcome this mismatch between seasonal energy supply and demand. To date, technical and economic investigations to meet any scale of energy storage are predominantly based on the integration of TES technologies including sensible, latent or thermochemical [5]. Presently, the unit cost to store thermal energy is higher due to the high cost of its components [6]. The main cost contributors to a TES system are storage media costs, tank, HTF, encapsulation cost, pumping cost and overhead costs [7]. Lazard [5] presented a levelized cost framework of storage in defined applications to identify the minimum costs per unit associated with the leading storage technologies, and the costing assumptions were derived from a robust survey of industry participants. Overall power plant efficiency can be improved while optimizing unit cost by using materials and system integration approaches which enable operation with large temperature swings. The same is true for the TES system and its components [8]. However, the advancement in thermal storage technologies face two major barriers to the market entry, i.e., process integration of TES with stable performance and the cost of the

---

Nomenclature

R	radius of storage tank (m)
R_{PCM}	radius of PCM (m)
H	height of storage tank (m)
t_c	cut-off time (s)
T	temperature (K)
V	volume (m^3)
H_{PCM}	PCM enthalpy (J/kg)
$T_{f,out}$	temperature of HTF at outlet (K)
$T_{f,inlet}$	temperature of HTF at inlet (K)
T_i	initial temperature (K)
T_{fi}	final temperature (K)
T_m	melting temperature (K)
T_c	critical cold temperature (K)
T_h	critical hot temperature (K)
X	fraction of molten PCM
X_{tc}	thermocline thickness (m)
h_v	volumetric heat transfer coefficient (W/m^{3}K)
$h_{v,s}$	volumetric heat transfer coefficient of SRS (W/m^{3}K)
$h_{v,PCM}$	volumetric heat transfer coefficient of PCM (W/m^{3}K)
A_s	surface area (m^2)
ΔX	control volume size (m)

ΔP	pressure drop (Pa)
G	mass flow rate per unit cross area (kg/m^2 s)
r	equivalent radius of storage material (m)
W_p	pumping work (J)
t_d	discharging time of energy (s)
$\dot{m}$	mass flow rate (kg/s)
Q_i	energy initially stored in tank, kJ
Q_f	thermal energy stored by HTF, kJ
Q_{SRS}	thermal energy stored by SRS, kJ
Q_{PCM}	thermal energy stored by PCM, kJ

Greek characters

μ	viscosity (kg/m s)
ρ	density (kg/m^3)
ε	porosity
η_d	discharge efficiency

Subscripts

PCM	phase change material
f	fluid
SRS	sensible rod structure

system [4].

The literature study shows that both sensible and latent heat TES systems have advantages and limitations. Sensible heat thermal energy storage (SHTES) systems are commercially available well developed technologies and use cheap naturally occurring materials like concrete, rocks etc. as a storage media [9]. SHTES systems have been studied by many researchers and it shows low degradation in performance over the discharging period with advantages in terms of robustness, reliability and reduced overall cost of the TES system [10]. However, low storage capacity per unit volume and the temperature drops at the end of discharging cycles make it less attractive [11]. Moreover, due to lower capacity factor of the sensible filler material, the size of tank required by thermocline unit is approximately equivalent to a two-tank TES system. This results in an insignificant difference of storage tank cost between thermocline SHTES and two tank TES system [12]. Most of the previous studies used a packed bed aggregate filler as a storage material which later on experiences a critical technical issue of thermal ratcheting, negatively affecting the operational life time and robustness of a TES system [13]. Therefore, Strasser et al. [10] suggested structured design of the sensible storage media. The use of structured sensible storage media has the advantages that it avoids thermal ratcheting and for a given volume it can accommodate more thermal energy even at higher temperatures [14].

On the other-hand, latent heat thermal energy storage systems look comparatively more attractive because of high storage capacity per unit volume with small temperature swings and isothermal features during charge/discharge cycles [15]. However, some limitations like high capacity cost per kWh, low thermal conductivity and unstable thermophysical properties under extended operational cycles make it less attractive. Moreover, the low heat transfer rates during heat recovery cycles due to the developing solid layer inside PCM, hinder its commercial scale application [16]. The phase change temperature (PCT) of latent heat storage material affects the outlet temperature of a TES system especially for an application specific process [17]. Abhiji et al. [18] investigated the mixtures of mannitol and galactitol as a potential PCM for use in medium temperature TES applications. The experimental studies carried out by the researchers suggested that D-Mannitol is the most suitable latent heat storage candidate for medium temperature applications (433–473 K); as it retains a large temperature difference of 405 K between its melting point and the decomposition

temperature [19].

The overall economic feasibility of a thermal storage unit depends heavily on the specific application and operational cycles [6]. The capacity cost of a TES system is evaluated based on the capital cost, operational costs of the storage system components and its life cycles [20]. The cost of latent heat TES systems are generally in the range of $12–57.3/kWh [6]. Whereas, the capacity cost of sensible heat TES using packed bed and structured storage material is evaluated to be $30/kWh and $34/kWh, respectively [10]. It heavily depends upon the application type, specific heat of storage media, number of charging/discharging cycles and the thermal insulation technique. Thaker et al. [8] used data-intensive bottom up models to evaluate the economic feasibility of sensible, latent and thermochemical TES units based on Monte Carlo simulations. They concluded that although the cost per kWh of a thermocline TES unit is relatively lesser than the other types, but still there is a substantial range of opportunity to cut investment costs and levelized cost of energy. The power needed to pump HTF contributes to the cost of a TES system too. Sagara et al. [21] concluded that the difference in pump energy between large sized and smaller storage materials becomes significant if the bed size is longer. The authors [11] experimentally studied TES using silicate rocks as storage material and reported that less than 1% pumping power is needed for a rock size of more than 10 mm. Maaliou and McCoy [22] proposed optimized design parameters for a longer packed bed column to make the TES cost effective in terms of pumping cost and the capital expenditures.

The techno-economic issues associated with sensible and latent heat TES systems need to be fixed before they are made abundantly available for commercial applications [23]. The hybrid combination of latent and sensible heat storage materials can create a useful effect to combine the advantages of these systems; and cope with the issues to some extent experienced by SHTES and LHTES [2]. The passive TES units using concrete as sensible storage media are usually implanted with tubular heat exchangers instigating increased heat transfer rates because of enhanced thermal conductivity and larger contact area between them. However, the temperature may vary during discharging cycles. This issue can be overcome by using PCMs but with lower heat exchange rates [24]. Zanganeh et al. [25] investigated the effect of different PCM heights placed above the layer of packed bed of rocks. They found that a suitable combination of phase change temperature and the heat of

fusion can act as a buffer to stabilize the fluid outlet temperature without significantly affecting its efficiency. Different configurations of a single TES unit using the idea of multi layered solid PCM was numerically studied by Galione et al. [26], and concluded that the sensible storage material in combination with multi layered PCM is a promising alternative for TES system.

The literature studies reveal that limited research has been carried out to investigate the hybrid effect of sensible-latent heat storage media on thermocline performance. To the best of authors' knowledge, till no work has been reported which focuses on thermo-economic assessment of one-tank thermocline TES configuration, using the concept of sensible structured material hybridized with PCM capsules for medium temperature applications. The aim of current work is to meet the economic requirements and optimize the thermal performance of a thermocline TES system by introducing a new type of combined sensible-latent heat TES configuration. The proposed thermocline TES configuration helps to counter the issues of thermal ratcheting, unstable fluid outlet temperature, higher thermocline degradation and quick temperature drops at the end of discharging cycles while optimizing the capacity cost ($/kWh).

2. Model formulation

In current study, the thermal performance of three different types of TES configurations are studied along with their cost analysis. The pure sensible heat TES, i.e., SRS configuration as can be seen in Fig. 1(a) consists of brick manganese rod structures filled as storage material. For pure latent heat TES, i.e., EPCM configuration, the tank is filled with encapsulated PCM capsules as storage material and is shown in Fig. 1(b). The proposed configuration which is the hybrid combination of the two configurations; having encapsulated PCM impregnated between SRS is shown in Fig. 1(c). The fluid flow path is of the same length as the tank height and the tank has distributors for radial uniform distribution of HTF at the inlet section of storage tank. The numerical model is developed using an energy balance method for the sensible and latent heat storage sections coupled with enthalpy method to study the influence of phase change temperature in the PCM. Moreover, a comprehensive cost model is formulated to evaluate the economic feasibility of the three types storage prototypes. It is based on direct cost and indirect costs incurred by the TES systems.
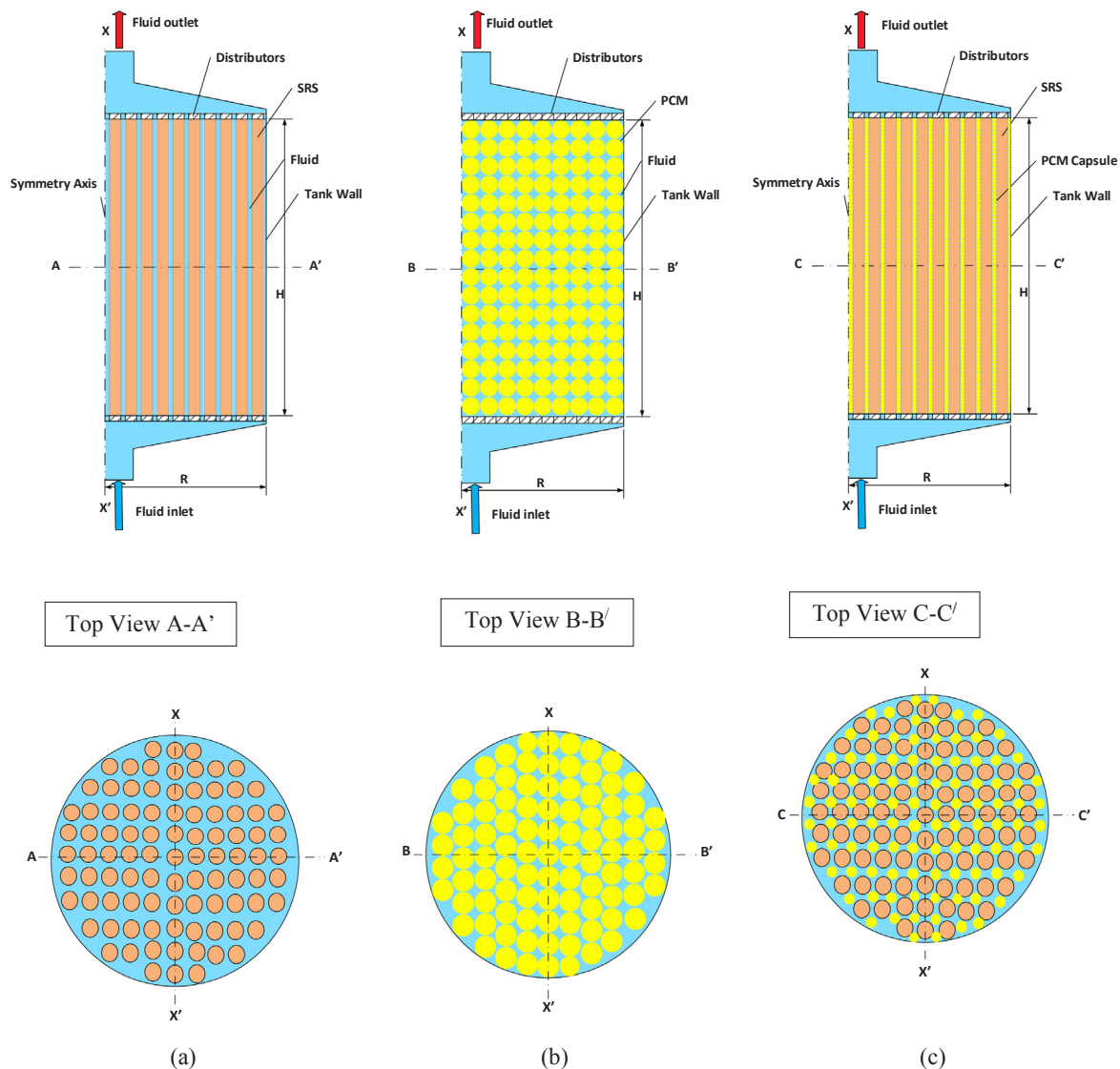

Fig. 1. Schematic of the three types of TES configurations (a) SRS (b) EPCM (c) HSRSEPCM.

2.1. Numerical energy model

The developed transient numerical model is evaluated using an energy balance method coupled with an enthalpy method governed by separate equations for fluid, sensible and latent heat storage media.

2.1.1. For fluid

The energy balance equation for fluid entering with a superficial velocity u at a temperature T_{in} in a control volume (A Δx) can be written as [27].

$$\frac{\partial}{\partial t}(A_f \Delta X \rho_f \ \varepsilon T_f) + \nabla \cdot (\rho_f \ \ u A_f \Delta X T_f) = \frac{h_{v,S} A_S}{C_{p,f}} \frac{\Delta X}{} (T_S - T_f) + S_1 \tag{1}$$

where S_1, is an added transient term taking into account the enthalpy changes in phase changing capsules because of the heat transfer with fluid.

$$S_t = \frac{\partial}{\partial t}\left(\frac{\rho_{PCM} A_{PCM} \ \Delta X H_{PCM}(1-\varepsilon)}{C_{p,f}}\right) \tag{2}$$

2.1.2. For sensible storage section

For sensible storage media the energy balance equation is written as [27].

$$\frac{\partial}{\partial t}(\rho_S(1-\varepsilon)C_{p,S} A_f \ \Delta X \ T_S) = h_{v,S} A_S \ \Delta X (T_f - T_S) \tag{3}$$

2.1.3. For latent heat storage section

The enthalpy equation for latent heat storage media is governed by [28].

$$\frac{\partial}{\partial t}(\rho_{PCM}(1-\varepsilon)H_{PCM}) = h_{v,PCM}(T_f - T_{PCM}) \tag{4}$$

where the value of H_{PCM} depends on the region in which it lies during solidification or melting and is a function of T_{PCM}.

$$H_{PCM} = \begin{cases} C_{ps,PCM} T_{PCM} & T_{PCM} \leqslant T_{sol} \\ C_{ps,PCM} T_{PCM} + \frac{L_{PCM}}{(T_{liq} - T_{sol})}(T_{PCM} - T_{sol}) & T_{liq} < T_{PCM} < T_{sol} \\ C_{ps,PCM}(T_m - T_i) + C_{pl,PCM}(T_{fi} - T_m) + L_{PCM} & T_{PCM} \geqslant T_{liq} \end{cases} \tag{5}$$

The pressure drop across TES tank is calculated using the correlation [29]

$$\Delta P = \frac{2(1-\varepsilon)H G^2}{r \varepsilon^3 \rho}\left(1.75 + 300\frac{\mu}{G r}\right)\Delta P = \frac{2(1-\varepsilon)H G^2}{r \varepsilon^3 \rho}\left(1.75 + 300\frac{\mu}{G r}\right) \tag{6}$$

$W_p = \int_0^{t_d} \frac{A\Delta pG}{\rho_f} dt$ The energy required to pump the HTF is evaluated by the relation [11]

$$W_p = \int_0^{t_d} \frac{A\Delta pG}{\rho_f} dt \tag{7}$$

The overall effectiveness of energy extracted from the thermal storage units during the discharging process is quantified by evaluating discharging efficiency. It is defined as the ratio between the amount of useful thermal energy recovered from TES tank during the discharging period to the maximum amount of energy stored initially before starting the discharging process [30]. It is governed by the relation as

$$\eta_d = \frac{\int_0^{t_c} \dot{m} C_p (T_{f,out} - T_{f,inlet}) dt}{Q_i} \tag{8}$$

where Q_i, the amount of thermal energy stored initially depends upon the configuration case and the type of storage filler material.

$$Q_i = \begin{cases} Q_f + Q_{SRS} & \text{For SRS configuration} \\ Q_f + Q_{PCM} + Q_{SRS} & \text{For HSRSEPCM configuration} \\ Q_f + Q_{PCM} & \text{For EPCM configuration} \end{cases} \tag{9}$$

where the energy stored in fluid Q_f, SRS filler Q_{SRS} and EPCM filler Q_{PCM} are calculated as

$$Q_f = (\rho_f V_f C_{p,f})(T_{fi} - T_i) \tag{10}$$

$$Q_{PCM} = (X\rho_l V_{PCM} L_{PCM}) + (\rho_s V_{PCM} C_{p,s}(T_m - T_i)) + (\rho_l V_{PCM} C_{p,l}(T_{PCM} - T_m)) \tag{11}$$

$$Q_{SRS} = (\rho_S V_S C_{p,S})(T_{fi} - T_i) \tag{12}$$

The practical usefulness of a thermal storage system is greatly governed by the threshold temperature of an application [31]. In the current study the amount of energy which is recovered above the threshold temperature, i.e., T_i – 32, is considered as useful and used to determine effective discharging efficiency (EDE) and effective discharging time (EDT).

Thermocline thickness is an important parameter to evaluate the overall discharging performance of a single thermal energy storage tank. It can be defined as the length of thermocline region covering the storage tank. In order to determine the thermocline thickness, it requires a continuous profile of temperature distribution [30].

$$X_{tc} = \begin{cases} H(T_h) - H(T_c) & (T_{f,inlet} \leqslant T_c) \& (T_{f,out} \geqslant T_h) \\ H(T_h) - 0 & (T_{f,inlet} > T_c) \\ H - H(T_c) & (T_{f,out} < T_h) \end{cases} \tag{13}$$

where T_c and T_h are the critical cold temperature and critical hot temperature. In current studies for the evaluation of thermocline thickness T_c and T_h are taken as 412 k and 468 k, respectively.

2.1.4. Initial and boundary conditions

The formulated equations for the numerical model are solved using suitable set of initial and boundary conditions. During discharging at the inlet section of the storage tank velocity and temperature are given while at outlet Neumann pressure and temperature are provided as boundary conditions. The well-insulated outer wall of tank assumes an adiabatic boundary condition. The tank is considered at an initial condition to be fully charged with thermal energy having sensible rod structures, PCM and the surrounding fluid at the same high temperature of 468 K within the entire tank.

(i) At inlet: At t> 0 $\quad T_f = 408$ K, $\quad u = 0.002$ m/s $\qquad (14)$

(ii) At symmetry axis: $\frac{dT_f}{dy} = 0, \quad \frac{du}{dy} = \frac{dv}{dy} = 0 \qquad (15)$

(iii) At outer wall: $\frac{dT_f}{dy} = 0, \quad \frac{dT_{PCM}}{dy} = 0, \quad \frac{dT_S}{dy} = 0, \quad u = v = 0 \qquad (16)$

(iv) At outlet: $\frac{dT_f}{dx} = 0, \quad \frac{dT_{PCM}}{dx} = 0, \quad \frac{dT_S}{dx} = 0, \quad P = 0 \qquad (17)$

2.1.5. Numerical methods

The formulated equations are evaluated numerically to study the thermocline behavior of the three TES configurations. The computational domain is taken as 2D axisymmetric having a height of 7.5 m and a radius of 2.5 m. All the three configurations use a porosity of 0.5 with SRS having the same radius of 0.04 m. The properties of filler materials and HTF are illustrated in Table 1. In order to verify the accuracy of the developed numerical model, a grid independency test was performed. The selected meshing grid is quadrilateral dominant having cells with a discretization size around 75 mm. The numerical model employed first order implicit scheme with Semi-Implicit Method for Pressure-Linked Equations (SIMPLE) method for the transient formulation of temporal

Table 1

Properties of the materials [18,32,33].

Material property	Value
Specific heat of SRS ($C_{p,s}$), J/kg K	1130
Density of brick manganese (ρ_s), kg/m^3	3000
Conductivity of brick manganese (K_s), W/m K	5.07
Density of HTF (ρ_f), kg/m^3	940
Conductivity of HTF (K_f), W/m K	0.10
Specific heat of HTF ($C_{p,f}$), J/kg K	2000
Viscosity of HTF (μ_f), kg/m s	4.90×10^{-04}
Melting point of D-Mannitol, (T_m)	438
Latent heat of D-Mannitol (L_{PCM}), J/kg	3.0×10^{05}
Specific heat of liquid D-Mannitol ($C_{pl,PCM}$), J/kg K	1310
Specific heat of solid D-Mannitol ($C_{ps,PCM}$), J/kg K	2360
Density of D-Mannitol (ρ_{PCM}), kg/m^3	1490
Conductivity of liquid D-Mannitol ($K_{l,PCM}$), W/m K	0.19
Conductivity of solid D-Mannitol ($K_{s,PCM}$), W/m K	0.11
Solidus Temperature of D-Mannitol (T_{sol}), K	435.15
Liquidus Temperature of D-Mannitol (T_{liq}), K	440.8

terms. The gravity direction is taken along the axial flow and first order upwind scheme is used with Least Square Cell based method for the spatial discretization of domain.

2.2. Cost model

The capital cost of a single thermocline TES unit is the summation of direct cost and indirect cost. In the current cost model using the same volume of tank for all the three configurations, direct cost consists of storage material cost, tank cost, encapsulation cost and miscellaneous expenditures. The estimation of indirect cost includes sales tax, engineering cost and contingency cost. The management costs are not considered in the current cost model because of uncertain practical situation of the projects. The per unit rates of the TES cost contributors considered to evaluate the cost model, are enlisted in Table 2.

The storage material cost includes the cost of encapsulated PCM, SRS, HTF or addition of these in case of combined sensible-latent heat TES and are evaluated by weight. The storage material cost C_{sm} for SRS is evaluated using the relation [10,34].

$$C_{sm} = (\rho_S(1 - \varepsilon)C^*_{SRS} + \rho_f \varepsilon C^*_f)\pi R^2 H \qquad (18)$$

where, C^*_{SRS} and C^*_f are per unit cost of solid rod structure and HTF, respectively. The storage material cost for EPCM configuration is given by the relation

$$C_{sm} = (\rho_{PCM}(1 - \varepsilon)C^*_{PCM} + \rho_f \varepsilon C^*_f)\pi R^2 H \qquad (19)$$

where C^*_{PCM}, is the per unit cost of PCM [17].

The storage material cost for the proposed hybrid configuration, i.e., HSRSEPCM is evaluated based on the mass occupied by storage fillers (PCM, SRS and HTF) and multiplying with the unit cost.

$$C_{sm} = \rho_{PCM} V_{PCM} C^*_{PCM} + \rho_S V_S C^*_{SRS} + \rho_f V_f C^*_f \qquad (20)$$

The cost of storage tank (C_{st}) is the summation of tank material cost [35], foundation cost and insulation cost [36], which is calculated based on the covered area [20].

$$C_{st} = \rho_{ss} H(\pi(R + W_t)^2 - \pi R^2)C^*_{ss} + \pi R^2 C''_F + 2\pi R H C''_{ins} \qquad (21)$$

where C^*_{SS}, C''_F, C''_{ins} are per unit expenses of stainless steel, foundation and insulation respectively. The encapsulation cost (C_{enc}) is evaluated using the relation [7]

$$C_{enc} = \left(\frac{R_{PCM}}{0.005}\right)^{0.3} C^*_{enc} \qquad (22)$$

The overhead cost includes the expenditures of electrical, piping, fitting, valves and instrumentation. It is assumed to be 10% of the total storage media cost and the storage tank cost [20].

The validity of current cost model is checked by comparing its

economic estimation with the same kind of studies from literature. By employing the above mentioned cost model methodology, the single tank TES system with structure sensible storage material exhibits a capacity cost of 35 $/kWh, which is close to 34 $/kWh as reported in the Ref. [10]. Also, the per unit rates of the components shown in Table 2 were employed for a two tank TES system by using the methodology reported by the author for base case total cost estimation [20]. The cost is evaluated to be 29 $/kWh, which is close to the benchmark value of 26.2 $/kWh. A little discrepancy is attributed to the difference in HTF and storage material costs suited for medium temperature applications.

3. Results and discussion

In this section, first, the validation of the numerical energy model is presented and then comparative performance analysis of the three types of TES systems is discussed. Moreover, economic feasibility of each TES system is presented with detailed cost analysis.

3.1. Model validation

The developed numerical energy model is validated using experimental data from two different studies. The numerical model was authenticated for the sensible heat storage section by comparing simulated results with the experimental study reported by Hänchen et al. [11]. The experimental data of pilot scale thermal storage setup using rocks as storage material is shown in Fig. 2(a). The formulated numerical model uses dimensions and properties taken from the previous work by the same research group [11,37]. The validity of the current model was confirmed for latent heat storage section of TES by comparing the simulation results with the experimental data published by Nallusamy et al. [38]. Their experimental prototype used capsules filled with paraffin wax as latent heat storage material and water was taken as heat transfer fluid The comparison of numerically calculated results and the experimental data indicates a reasonable trend as shown in Fig. 2, giving an average of 3.16% and 7.02% for sensible and latent heat sections respectively. The difference in error may be attributed to the simplification of the model neglecting inlet effects of HTF at the entry of tank. Also because the conductivity of capsule film thickness is ignored in the current numerical model, while it is included in the experimental data. The uncertainty about exact placement of thermocouples in the experimental setup also adds to the error. The overall agreement between the experimental and the numerical results endorses validity of the numerical model. This forms a foundation for the comparative numerical analysis, which is presented in the results section.

3.2. Performance analysis

The analysis presented in this section indicates that an efficient TES is accomplished by reduced thermocline degradation and the higher stratification factor causing improved heat transfer [27]. An important index to evaluate the qualitative performance of a thermocline TES system is to investigate the shape of temperature profiles during the

Table 2

Per unit rates of the cost contributors to a thermocline TES system.

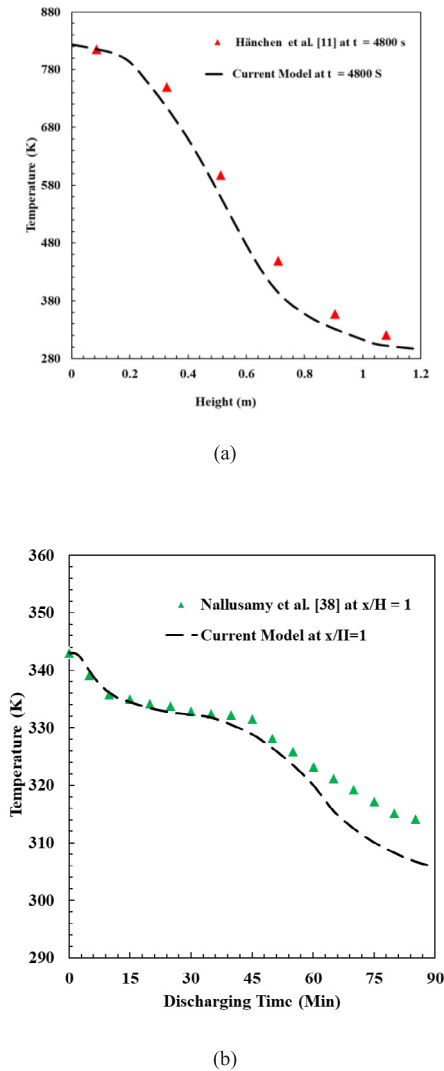| Cost contributor	Cost per unit
PCM ($/t)	998
SRS ($/t)	69
HTF ($/t)	952
Stainless steel (316 ss) ($/t)	2812
Encapsulation of PCM ($/t)	771
Insulation ($/m^2)	206
Foundation ($/m^2)	1199

(a)

(b)

Fig. 2. Comparison between numerical results and experimental data for (a) Sensible heat storage section (b) Latent heat storage section.

discharging process. A step function is usually desirable for an ideal temperature profile, which indicates that the thermocline region should have minimal thickness. The lower the thermocline thickness, the higher the heat transfer between fluid and the storage media. This results into reduced mixing of hot and cold regions of the storage tank. To illustrate this point, consider comparative discharging fluid temperature profiles of SRS, EPCM and HSRSEPCM as shown in Fig. 3. The fluid temperature profiles in EPCM configuration maintain a thin "S" shape with the thermocline region occupying only a small section of the tank height due to excellent stratification in the packed bed of PCM. Whereas, the temperature profiles in SRS configuration show the least sharp "S" shape with thermocline layer expanding to fill more than half of the tank height. This is due to lower heat exchange rates with the walls of the sensible rod structure. HSRSEPCM configuration shows the intermediate performance of thermocline temperature profiles. The impregnation of PCM capsules between SRS increase the stratification factor and results into increased heat transfer rates with the storage material relative to the SRS configuration. However, EPCM TES configuration exhibit superior thermocline characteristics for the same size of storage tank due to higher storage density.

For the convenience of thermocline analysis, the temperature profiles of fluid at $X = H/2$ for the considered configurations as a function of discharge time is chosen as the representative profile. The results in Fig. 4 show that for SRS case the temperature of TES system starts to

decrease only after 12 min (Min) and becomes fully discharged after 165 Min when the temperature reaches 408 K. For EPCM case, the TES unit shows higher performance than the both SRS and HSRSEPCM exhibiting higher discharge time. While the hybrid configuration in HSRSEPCM case shows improved discharge performance than SRS, where the latent heat of PCM helps to elongate the EDT around phase transition temperature of the PCM, i.e., 438 K. After that, the temperature profile falls quickly due to the solidification of PCM capsules. For instance, after 80 Min of discharge the temperature of fluid at the center of tank for SRS, EPCM and HSRSEPCM is 419 K, 467 K and 436 K respectively.

Comparative thermal performance and the formation of thermal gradient along the flow direction of a TES system can be more clearly explained in terms of thermocline thickness profiles. Fig. 5 shows the thickness of thermocline regions predicting the formation and degradation of thermal gradient. The TES systems with the lower thermocline thickness help to maintain the fluid outlet temperature at a higher value. The results in Fig. 5 illustrate that initially there is a sharp increment in thermocline region and after some discharging time when the cold inlet HTF starts to gain thermal energy, the growth in thermocline thickness is slowed down. The maximum value is attained when the thermocline region reaches at outlet and thereafter, it has a linear decrease in thermocline thickness. Accordingly, the maximum thermocline thicknesses achieved for SRS, EPCM, HSRSEPCM are 6.19 m, 3.22 m, 5.22 m at the discharge period of 50 Min, 120 Min and 75 Min respectively.

The performance in terms of total energy extracted from different TES configurations during the discharge process is shown in Fig. 6. The rate of thermal energy discharge is presented by the slope of curve, which is a measure of the dynamic characteristic of a TES unit. The results show that EPCM attains the highest performance followed by HSRSEPCM. The SRS configuration exhibit lowest performance. This can be attributed to the reason that it possesses lowest storage capacity and the availability of heat driving force, arising due to temperature difference between filler material and HTF. Moreover, that the results show that after a discharging period of 210 Min, the energy recovered from TES prototypes for SRS, EPCM and HSRSEPCM are 92%, 84% and 90%, respectively.
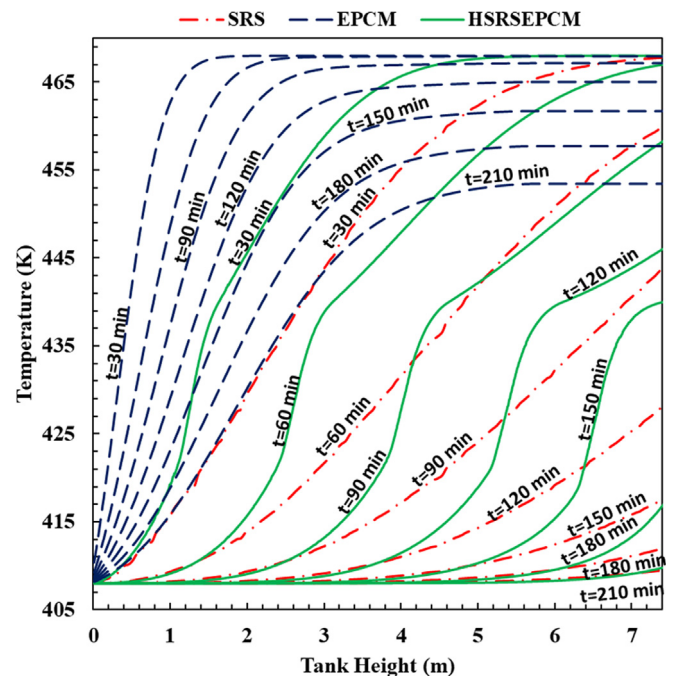

Fig. 3. Temperature distribution of fluid along axial direction at different discharging moments for SRS, EPCM and HSRSEPCM.
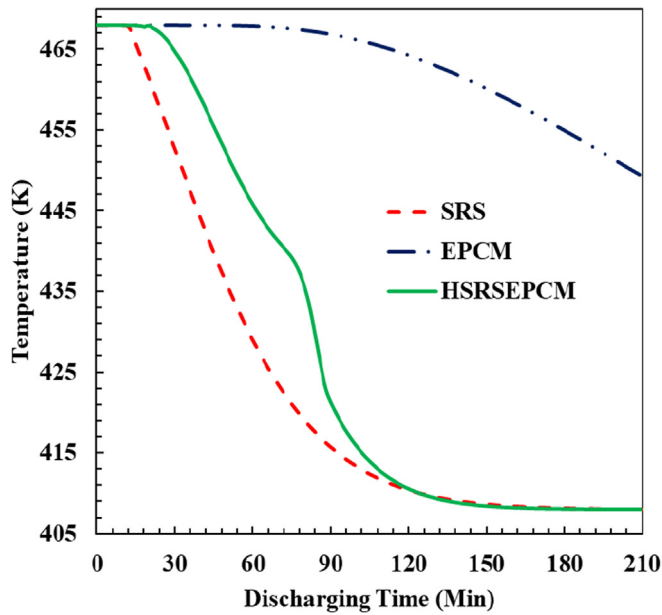
Fig. 4. Temperature profiles of fluid for SRS, EPCM and HSRSEPCM at $X = $ H/2 as a function of discharging time.
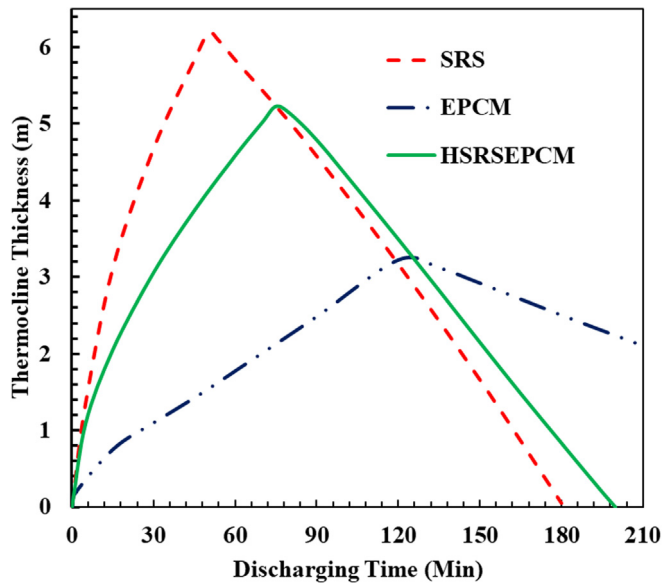

Fig. 5. Thermocline thickness profiles for SRS, EPCM and HSRSEPCM as a function of discharging time.

Fig. 7 shows that initially the discharge efficiency for all three cases increases linearly for several minutes, then the increment becomes slow because the thermocline region approaches at the outlet of TES system. The efficiency is said to be 100% when the stored energy is completely released. The results show that the maximum EDE achieved for EPCM is 95% followed by HSRSEPCM with 87% and the least for SRS case is 76%. Moreover, it is also observed that the discharging efficiency increases first linearly higher for SRS as compared to that of the other two cases. This is because the HTF at outlet takes shorter time to fall below the threshold temperature resulting in reduced EDT. The EDT is calculated to be 105 Min, 167 Min and 254 Min for SRS, HSRSEPCM and EPCM, respectively.

Comparative pump energy required to overcome the pressure drop for the three configurations is shown in Fig. 8. For the SRS case, filled with only rod structure as storage material; does not have obstruction within the storage media for the fluid flow resulting in the lowest
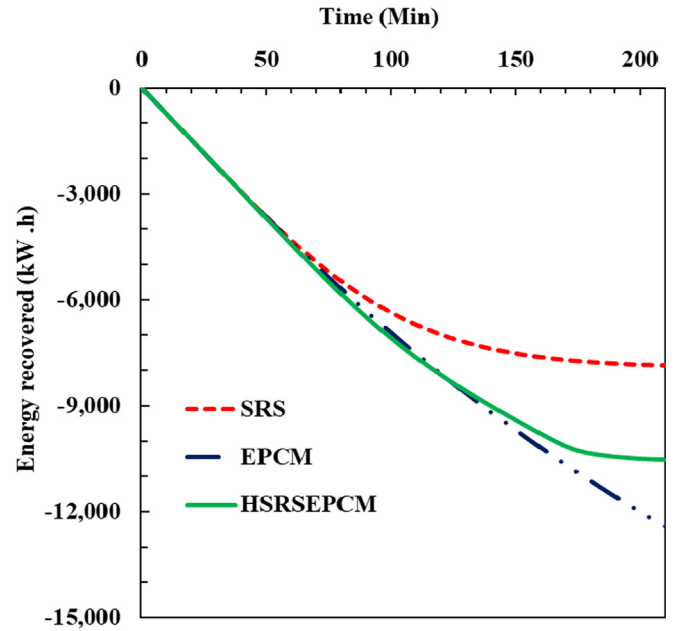

Fig. 6. Total energy recovered from the TES systems during discharging process for SRS, EPCM and HSRSEPCM configurations.

pressure drop. In this case the pump energy can be ignored even for larger sizes of TES tank. Whereas, the EPCM configuration shows very higher pressure drop of 8 kPa as compared to the other two cases. This adds more to the total cost of the system and thus making the option less favorable to be used as TES. The proposed HTES tank configuration needs only 2481 kJ of pump work to over the pressure drop which is higher than SRS case but lower than that of EPCM case. key performance parameters of the three types of TES configurations are shown in Table 3.

3.3. Cost analysis

An important index to predict the economic effectiveness of a TES unit is capacity cost per kWh. It is evaluated using the total stored energy available to be extracted during the discharging process and the
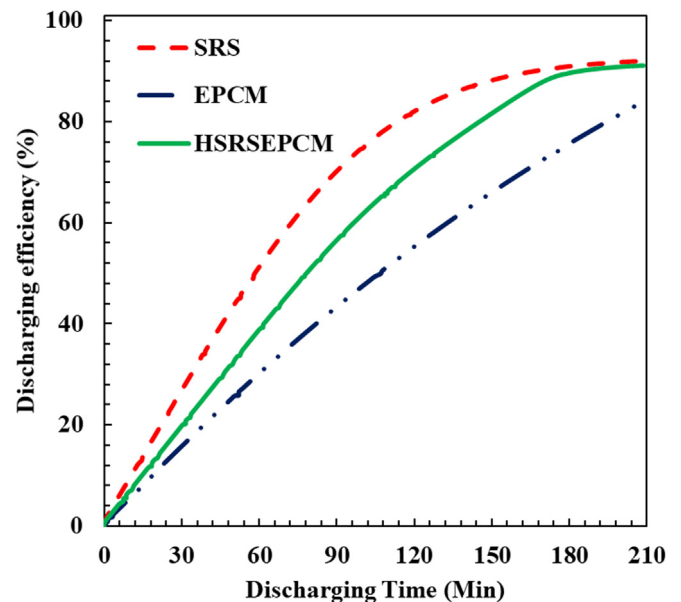

Fig. 7. Comparative discharging efficiency of SRS, EPCM and HSRSEPCM as a function of time.
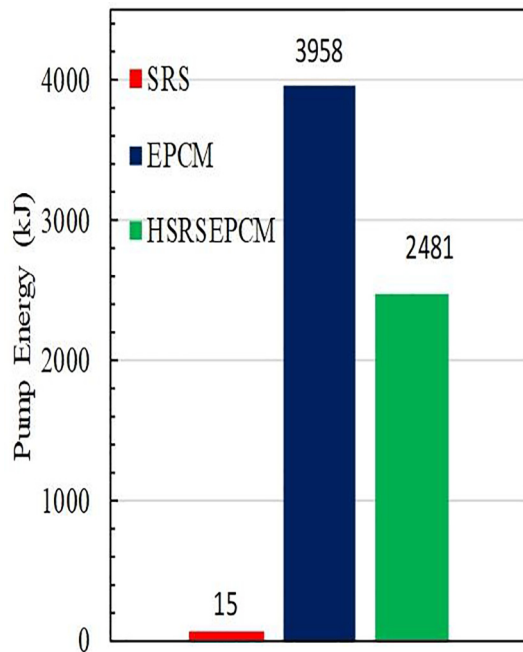
Fig. 8. Comparative pump energy utilization for SRS, EPCM and HSRSEPCM to overcome the pressure drop.

Table 3

Comparative key performance parameters of the three types of TES configurations.

TES type	Pressure Drop (kPa)	Max. Thermocline Thickness (m)	EDT (Min)	EDE (%)
SRS	0.03	6.19	105	76
EPCM	8	3.22	254	95
HSRSEPCM	5.01	5.22	167	87

overall installation cost of the TES unit [20]. As per the cost model mentioned in the previous Section 2.1; the component cost details and the total capital cost for the SRS, EPCM and HSRSEPCM TES configurations are presented in Fig. 9. Using the same size of TES unit, the highest installation cost is for EPCM configuration of 624,540 $, followed by HSRSEPCM, SRS costing 430,441$, and 300,028 $, respectively. The calculations show that the proposed configuration i.e. HSRSEPCM is 30% more expensive than SRS configuration but 45% more cheap than EPCM configuration. The overhead costs take into account the expenditures of electrical, piping, fitting, valves and instrumentation cost. Whereas, the indirect cost includes engineering cost, sales tax and contingency cost.

Fig. 10(a) and (b) shows total storage capacity and storage capacity per unit volume of three different types of TES configurations, respectively. The results indicate that EPCM case has 42% and 22% higher total storage capacity than SRS and HSRSEPCM, respectively because of comparatively higher storage density of the PCM. But the higher capacity cost as indicated in Fig. 11 for EPCM configuration, i.e., 42 ($/kWh), makes it least favorable option among the studied configurations in the prospect of economic feasibility. The SRS configuration filled with only sensible material has the lowest capacity cost of 35 ($/kWh) but exhibit lower storage capacity of 8547 kWh. Whereas, HSRSEPCM prototype possesses slightly higher capacity cost of 37 ($/kWh) but shows a reasonable storage capacity of 11,562 kWh as compared to SRS storage prototype. Fig. 10(b) shows that the SRS configuration exhibits a storage density of only 58 kWh/m^3, which is 42.5% lower than EPCM configuration. This means it requires large volume of tank which adds significantly to the overall cost of system; as

the tank cost contribution is almost 50% of the overall SRS system cost. Whereas, HSRSEPCM possesses a storage capacity of 78.5 kWh/m^3. This is because the introduction of PCM capsules between SRS increases the maximum storage density of thermocline TES system.

In the previous sections first performance indices of the considered TES prototypes are analyzed and then their economic feasibility is presented. In order to come up with a viable TES solution, its necessary to consider both aspects i.e. thermal performance and the costs of the system. Pure sensible heat TES type, i.e., SRS configuration is the cheapest but the storage capacity and performance indicators are not encouraging. Whereas, pure latent heat TES type, i.e., EPCM configuration shows superior thermocline performance but the higher capacity cost and pumping costs make it less favorable option. Therefore, the hybrid TES configuration filled with PCM together with the
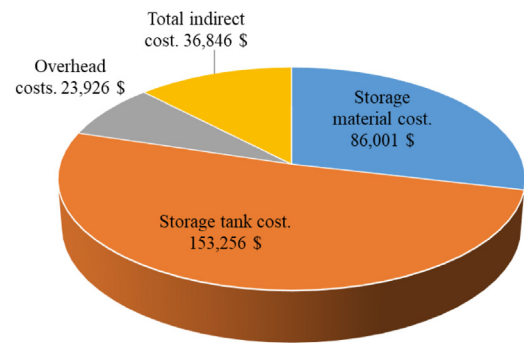
(a)
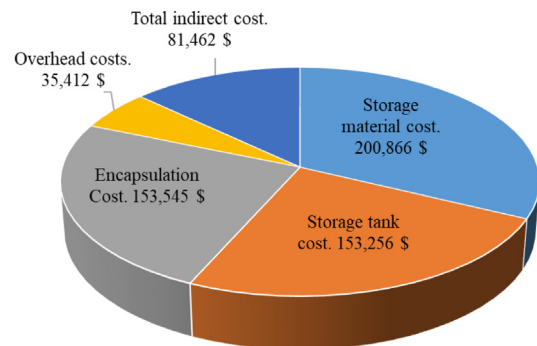
(b)
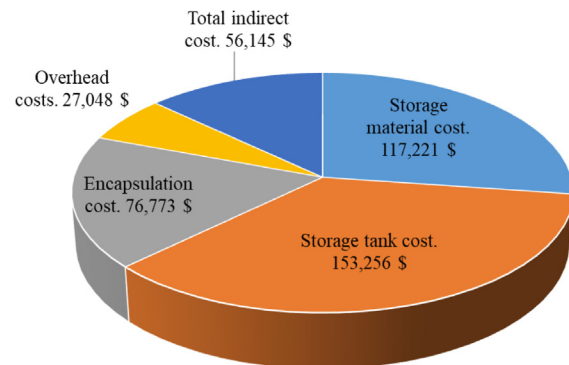
(c)

Fig. 9. Components costs of three different types of TES configurations (a) SRS (b) EPCM (c) HSRSEPCM.
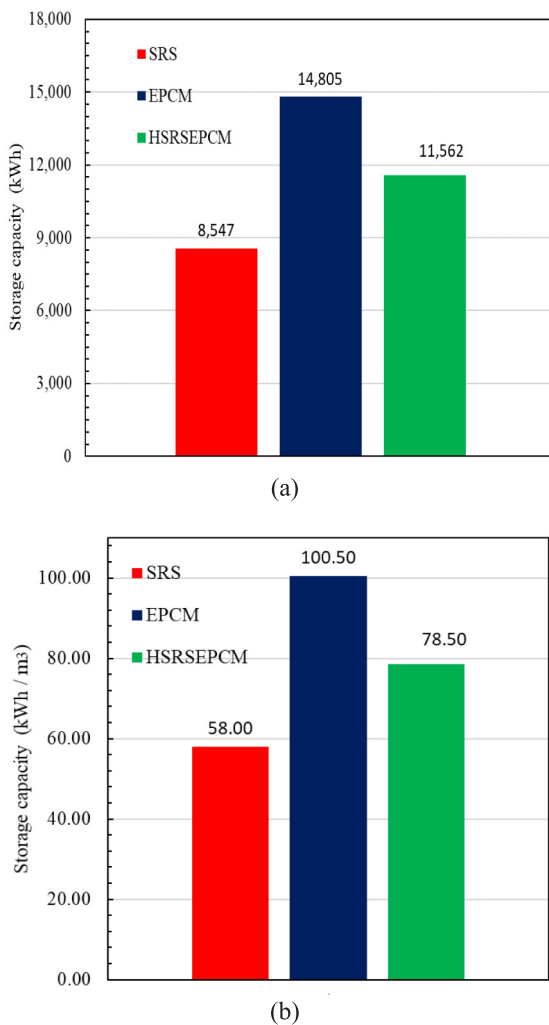
Fig. 10. Comparative storage capacity of three different types of TES configurations (a) Total storage capacity (b) storage capacity per unit volume.
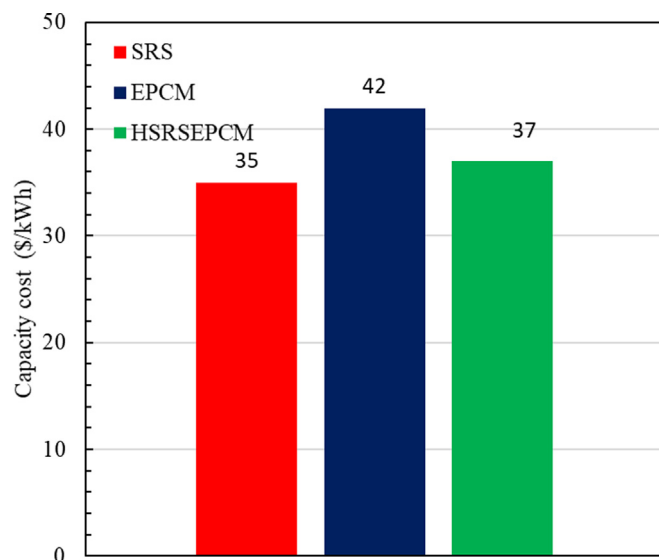

Fig. 11. Comparative capacity cost ($/kWh) of three different types of TES configurations SRS, EPCM and HSRSEPCM.

inclusion of a cheaper structured material, offer a comparatively efficient and cost-effective thermal storage alternative. However, efforts should still be made to develop countermeasures for the correct usage of PCM together with sensible material such that majority of it can effectively undergo the phase change. This is the main focus of next phase of ongoing research in which parametric studies of the proposed hybrid TES will be presented for optimum design by using multi-stage PCM capsules between SRS.

4. Conclusions

The main focus of the work is to evaluate performance indexes of the three different types of TES systems and to find out the performance optimized solution which is also cost effective. In current study, a new hybrid configuration of combined sensible-latent heat TES is presented to avoid the issues of thermal ratcheting and temperature drops at the end of discharging cycles. A comparative thermal performance analysis is performed using numerical simulations based on Schumann model equations governed by energy balance method coupled with enthalpy technique. The proposed configuration, i.e., HSRSEPCM is compared performance wise and economically with the other two TES configurations. Important findings from the current study can be drawn as follows:

- EPCM configuration shows the best thermocline temperature profiles followed by the HSRSEPCM configuration, while SRS exhibits the weakest thermocline performance. However, the economic analysis shows that SRS is the cheapest while EPCM is the most expensive configuration.
- SRS discharges quickly at the end of discharging cycles, while in HSRSEPCM configuration the impregnation of PCM capsules between SRS structure helps to improve EDT around its PCT.
- The performance results show that the maximum EDE and thermocline thickness achieved for EPCM, SRS, HSRSEPCM are 95%, 87%, 76% and 3.22 m, 5.22 m, 6.19 m, respectively.
- SRS configuration exhibits a storage capacity of only 58 kWh/m^3 requiring large volume of tank. Whereas, HSRSEPCM shows a storage capacity of 78.5 kWh/m^3, which is 26% higher than SRS configuration and 22% lower than EPCM configuration.
- Higher pumping work of 3958 kJ is required for EPCM configuration than SRS and HSRSEPCM configuration, which require only 15 kJ and 2481 kJ, respectively.
- The capital cost of the HSRSEPCM is 30% higher than that of SRS however, it is 45% more cheap than EPCM configuration.
- Moreover, the cost model evaluated that EPCM possesses the highest capacity cost of $42/kWh followed by HSRSEPCM, SRS exhibiting $37/kWh and $35/kWh, respectively.

Therefore, it is concluded from the current study that the combined-sensible latent heat TES configuration is performance wise more optimized and cost-competitive among the considered thermocline storage prototypes for the same design requirements and operating conditions. However, more work is needed to explore the full potential of hybrid TES configuration for medium temperature applications.

Declaration of interests

None declared.

Acknowledgments

of China (No. 51721004) and the 111 Project (B16038).

Appendix A. Supplementary data

Supplementary data to this article can be found online at https://doi.org/10.1016/j.enconman.2019.03.040.

References

[1] Kılkış Ş, Krajačić G, Duić N, Rosen MA, Al-Nimr MA. Advancements in sustainable development of energy, water and environment systems. Energy Convers Manag 2018;176:164–83. https://doi.org/10.1016/j.enconman.2018.09.015.

[2] Pelay U, Luo L, Fan Y, Stitou D, Rood M. Thermal energy storage systems for concentrated solar power plants. Renew Sustain Energy Rev 2017;79:82–100. https://doi.org/10.1016/j.rser.2017.03.139.

[3] Jiménez-Arreola M, Pili R, Dal Magro F, Wieland C, Rajoo S, Romagnoli A. Thermal power fluctuations in waste heat to power systems: an overview on the challenges and current solutions. Appl Therm Eng 2018;134:576–84. https://doi.org/10.1016/j.applthermaleng.2018.02.033.

[4] Gibb D, Johnson M, Romaní J, Gasia J, Cabeza LF, Seitz A. Process integration of thermal energy storage systems – evaluation methodology and case studies. Appl Energy 2018;230:750–60. https://doi.org/10.1016/j.apenergy.2018.09.001.

[5] Lazard. Lazard's levelised cost of storage v2.0. Clim Policy 2016;6:600–6. https://doi.org/10.1080/14693062.2006.9685626.

[6] Zhou D, Zhao CY, Tian Y, Lott MC, Kim S-I, Eames P, et al. Technology Roadmap. Springer Reference 2013;92:24. https://doi.org/10.1007/SpringerReference_7300.

[7] Nithyanandam K, Pitchumani R. Cost and performance analysis of concentrating solar power systems with integrated latent thermal energy storage. Energy 2014;64:793–810. https://doi.org/10.1016/j.energy.2013.10.095.

[8] Thaker S, Olufemi Oni A, Kumar A. Techno-economic evaluation of solar-based thermal energy storage systems. Energy Convers Manag 2017;153:423–34. https://doi.org/10.1016/j.enconman.2017.10.004.

[9] Jemmal Y, Zari N, Maaroufi M. Thermophysical and chemical analysis of gneiss rock as low cost candidate material for thermal energy storage in concentrated solar power plants. Sol Energy Mater Sol Cells 2016;157:377–82. https://doi.org/10.1016/j.solmat.2016.06.002.

[10] Strasser MN, Selvam RP. A cost and performance comparison of packed bed and structured thermocline thermal energy storage systems. Sol Energy 2014;108:390–402. https://doi.org/10.1016/j.solener.2014.07.023.

[11] Hänchen M, Brückner S, Steinfeld A. High-temperature thermal storage using a packed bed of rocks – heat transfer analysis and experimental validation. Appl Therm Eng 2011;31:1798–806. https://doi.org/10.1016/j.applthermaleng.2010.10.034.

[12] Libby C. Solar thermocline storage systems: preliminary design study. Palo Alto, CA: Electr Power Res Institute; 2010.

[13] Flueckiger SM, Yang Z, Garimella SV. Thermomechanical simulation of the solar one thermocline storage tank. J Sol Energy Eng 2012;134:041014https://doi.org/10.1115/1.4007665.

[14] Abarr M, Geels B, Hertzberg J, Montoya LD. Pumped thermal energy storage and bottoming system part A: concept and model. Energy 2017;120:320–31. https://doi.org/10.1016/j.energy.2016.11.089.

[15] Li X, Ma T, Liu J, Zhang H, Wang Q. Pore-scale investigation of gravity effects on phase change heat transfer characteristics using lattice Boltzmann method. Appl Energy 2018;222:92–103. https://doi.org/10.1016/j.apenergy.2018.03.184.

[16] Elfeky KE, Ahmed N, Wang Q. Numerical comparison between single PCM and multi-stage PCM based high temperature thermal energy storage for CSP tower plants. Appl Therm Eng 2018;139:609–22. https://doi.org/10.1016/j.applthermaleng.2018.04.122.

[17] Pereira da Cunha J, Eames P. Thermal energy storage for low and medium temperature applications using phase change materials – a review. Appl Energy 2016;177:227–38. https://doi.org/10.1016/j.apenergy.2016.05.097.

[18] Abhiji P, Shi L, Bielawski CW. A eutectic mixture of galactitol and mannitol as a

phase change material for latent heat storage. Energy Convers Manag 2015;103:139–46. https://doi.org/10.1016/j.enconman.2015.06.013.

[19] Singh RP, Kaushik SC, Rakshit D. Melting phenomena in a finned thermal storage system with graphene nano-plates for medium temperature applications. Energy Convers Manag 2018;163:86–99. https://doi.org/10.1016/j.enconman.2018.02.053.

[20] Glatzmaier G. Developing a cost model and methodology to estimate capital costs for thermal energy storage. Nrel/Tp-5500-53066 2011:21.

[21] Sagara K, Nakahara N. Thermal performance and pressure drop of rock beds with large storage materials. Sol Energy 1991;47:157–63. https://doi.org/10.1016/0038-092X(91)90074-7.

[22] Maaliou O, McCoy BJ. Optimization of thermal energy storage in packed columns. Sol Energy 1985;34:35–41. https://doi.org/10.1016/0038-092X(85)90090-8.

[23] Ahmed N, Elfeky KE, Wang Q. Comparative thermo-economic analysis of structured thermocline combined sensible-latent heat thermal energy storage systems for medium temperature applications. 13th Conf Proc SDEWES20180255 2018.

[24] Alva G, Liu L, Huang X, Fang G. Thermal energy storage materials and systems for solar energy applications. Renew Sustain Energy Rev 2017;68:693–706. https://doi.org/10.1016/j.rser.2016.10.021.

[25] Zanganeh G, Commerford M, Haselbacher A, Pedretti A, Steinfeld A. Stabilization of the outflow temperature of a packed-bed thermal energy storage by combining rocks with phase change materials. Appl Therm Eng 2014;70:316–20. https://doi.org/10.1016/j.applthermaleng.2014.05.020.

[26] Galione PA, Perez-Segarra CD, Rodriguez I, Oliva A, Rigola J. Multi-layered solid-PCM thermocline thermal storage concept for CSP plants. Numerical analysis and perspectives. Appl Energy 2015;142:337–51. https://doi.org/10.1016/j.apenergy.2014.12.084.

[27] Van Lew JT, Li P, Chan CL, Karaki W, Stephens J. Analysis of heat storage and delivery of a thermocline tank having solid filler material. J Sol Energy Eng 2011;133:021003https://doi.org/10.1115/1.4003685.

[28] Felix Regin A, Solanki SC, Saini JS. An analysis of a packed bed latent heat thermal energy storage system using PCM capsules: numerical investigation. Renew Energy 2009;34:1765–73. https://doi.org/10.1016/j.renene.2008.12.012.

[29] Chandra P, Willits DH. Pressure drop and heat transfer characteristics of air-rockbed thermal storage systems. Sol Energy 1981;27:547–53. https://doi.org/10.1016/0038-092X(81)90050-5.

[30] Xu C, Wang Z, He Y, Li X, Bai F. Sensitivity analysis of the numerical study on the thermal performance of a packed-bed molten salt thermocline thermal storage system. Appl Energy 2012;92:65–75. https://doi.org/10.1016/j.apenergy.2011.11.002.

[31] Merlin K, Soto J, Delaunay D, Traonvouez L. Industrial waste heat recovery using an enhanced conductivity latent heat thermal energy storage. Appl Energy 2016;183:491–503. https://doi.org/10.1016/j.apenergy.2016.09.007.

[32] Singh H, Saini RP, Saini JS. A review on packed bed solar energy storage systems. Renew Sustain Energy Rev 2010;14:1059–69. https://doi.org/10.1016/j.rser.2009.10.022.

[33] Kumaresan G, Velraj R, Iniyan S. Thermal analysis of D-mannitol for use as phase change material for latent heat storage. J Appl Sci 2011;11:3044–8. https://doi.org/10.3923/jas.2011.3044.3048.

[34] Shenzhen Enesoon Science & Technology Co., Ltd, http://www.enesoon.com.cn/case1-detailed.asp?id = 140 [Accessed 05 March 2018]. n.d.

[35] http://www.meps.co.uk/Stainless%20price-asia.htm [Accessed 10 March 2018]. n.d.

[36] Kelly B, Kearney D. Thermal Storage Commercial Plant Design Study for a 2-Tank Indirect Molten Salt System Final Report. National Renewable Energy Laboratory (NREL); 2006. p. 1–32.

[37] Meier A, Winkler C, Wuillemin D. Experiment for modelling high temperature rock bed storage. Sol Energy Mater 1991;24:255–64. https://doi.org/10.1016/0165-1633(91)90066-T.

[38] Nallusamy N, Sampath S, Velraj R. Experimental investigation on a combined sensible and latent heat storage system integrated with constant/varying (solar) heat sources. Renew Energy 2007;32:1206–27. https://doi.org/10.1016/j.renene.2006.04.015.